Chemical Senses, 2016, Vol 41, 123–133
doi:10.1093/chemse/bjv065
Original Article
Advance Access publication October 28, 2015

Original Article

Changes in Olfactory Sensory Neuron Physiology and Olfactory Perceptual Learning After Odorant Exposure in Adult Mice

Marley D. Kass, Stephanie A. Guang, Andrew H. Moberly and John P. McGann

Behavioral & Systems Neuroscience Section, Department of Psychology, Rutgers University, 152 Frelinghuysen Road, Piscataway, NJ 08854, USA

Correspondence to be sent to: John P. McGann, Department of Psychology, Rutgers University, 152 Frelinghuysen Road, Piscataway, NJ 08854, USA. e-mail: john.mcgann@rutgers.edu

Accepted 13 October 2015.

Abstract

The adult olfactory system undergoes experience-dependent plasticity to adapt to the olfactory environment. This plasticity may be accompanied by perceptual changes, including improved olfactory discrimination. Here, we assessed experience-dependent changes in the perception of a homologous aldehyde pair by testing mice in a cross-habituation/dishabituation behavioral paradigm before and after a week-long ester-odorant exposure protocol. In a parallel experiment, we used optical neurophysiology to observe neurotransmitter release from olfactory sensory neuron (OSN) terminals in vivo, and thus compared primary sensory representations of the aldehydes before and after the week-long ester-odorant exposure in individual animals. Mice could not discriminate between the aldehydes during pre-exposure testing, but ester-exposed subjects spontaneously discriminated between the homologous pair after exposure, whereas home cage control mice cross-habituated. Ester exposure did not alter the spatial pattern, peak magnitude, or odorant-selectivity of aldehyde-evoked OSN input to olfactory bulb glomeruli, but did alter the temporal dynamics of that input to make the time course of OSN input more dissimilar between odorants. Together, these findings demonstrate that odor exposure can induce both physiological and perceptual changes in odor processing, and suggest that changes in the temporal patterns of OSN input to olfactory bulb glomeruli could induce differences in odor quality.

Key words: odorant exposure, olfactory sensory neuron, optical imaging, perceptual learning, sensory enrichment, synaptopHluorin

Introduction

The olfactory system can adapt to a constantly changing olfactory environment to maximize the detection and discrimination of frequently encountered or novel odor stimuli. In this dynamic sensory system, the first stage of stimulus processing takes place in the olfactory bulb, where neural representations of odor stimuli are shaped by complex and highly plastic circuitry before being communicated to other brain regions. Odor codes in the olfactory bulb correlate with the perception of odor quality (Malnic et al. 1999; Linster et al. 2001; Youngentob et al. 2006; Mandairon and Linster 2009), and both odor perception (Dalton and Wysocki 1996; Mandairon et al. 2006c) and olfactory bulb signal processing (Buonviso et al. 1998; Buonviso and Chaput 2000; Fletcher and Wilson 2003; Mandairon et al. 2008) are easily modified by olfactory experience. Consequently, an extensive series of studies have sought to correlate experience-dependent changes in odor perception with corresponding changes in early olfactory circuitry.

Previous work has shown that initially indiscriminable odorant pairs can become discriminable after a period of exposure to a chemically- and perceptually-different odorant (Mandairon et al. 2006b). This effect is robust and has motivated recent clinical trials using odor exposure as a therapy for anosmia (Damm et al.

2014; Altundag et al. 2015), because of the possibility that exposure therapy could enhance degraded sensory inputs at the level of the primary sensory neurons or evoke downstream plasticity that facilitates the interpretation of the degraded input itself (Czarnecki et al. 2012). The neural mechanisms underlying these perceptual effects are increasingly understood, and likely caused by experience-dependent alterations within the inhibitory circuitry of the olfactory bulb (Mandairon et al. 2008; Mandairon and Linster 2009). Passive exposure to olfactory stimuli promotes survival of inhibitory, adult-born interneurons in the glomerular and granule cell layers of the olfactory bulb and reduces cell death (Woo et al. 2006; Bovetti et al. 2009; Bonzano et al. 2014). Exposure-induced perceptual learning requires neurogenesis of olfactory bulb granule cells (Moreno et al. 2009), as well as norepinephrine-modulated fine-tuning of sensory processing in the inhibitory bulbar circuitry (Moreno et al. 2012; Vinera et al. 2015). Olfactory sensory enrichment also enhances GAD67 (Bovetti et al. 2009) and tyrosine hydroxylase (Bonzano et al. 2014) expression in juxtaglomerular (JG) cells involved in multiglomerular communication. The changes in bulbar neurogenesis and neurochemistry that are observed after a period of exposure are accompanied by an enhancement of odorant-evoked activity in JG (Woo et al. 2007) and granule (Mandairon et al. 2008) cell populations. However, these data do not exclude the possibility of plasticity in the odor-response properties of the olfactory epithelium, which would result in experience-dependent changes in the sensory input to all olfactory processing regions.

Olfactory transduction occurs in the olfactory epithelium, where olfactory sensory neurons (OSNs) physically contact olfactory stimuli in the external environment. Their axons travel back to the brain through the cribiform plate and thus constitute the primary sensory input to the olfactory bulb. The survival and density of OSNs in the epithelium can be influenced by olfactory experience (Watt et al. 2004; Cavallin et al. 2010). Moreover, OSN projections to their target glomeruli in the olfactory bulb are highly dependent on experience and can be altered through enriched (Kerr and Belluscio 2006; Valle-Leija et al. 2012) and deprived (Zou et al. 2004; Kass et al. 2013c) olfactory environments, both in the developing and the adult olfactory system. Odorant exposure alters the number of OSNs expressing a given odor receptor and can increase expression of odor receptor mRNA and associated transduction proteins like CNGA2 and phosphodiesterase 1C, which can result in increased sensitivity to odors and faster odor transduction kinetics (Cadiou et al. 2014).

Testing the role of OSN plasticity in exposure-induced perceptual change has proved challenging. Unlike the exposure-induced changes in the bulbar inhibitory networks, exposure-induced plasticity in OSNs is usually exclusive to OSNs expressing the cognate odorant receptor for the exposure odorant. After long-term exposure, OSN population-level electro-olfactogram (EOG) responses exhibit enhanced sensitivity to an exposed odorant, but not to an unexposed odorant (Wang et al. 1993). Lyral exposure induces dramatic molecular and physiological changes in OSNs expressing its cognate MOR23 receptor, but acetophenone exposure has no effect on these neurons (Cadiou et al. 2014). Seven days of exposure to an ester odorant selectively reduces transmitter release from the olfactory nerve evoked by the same ester and also enhances odorant-response-selectivity of OSNs, but has little or no effect on responses to nonesters (Kass et al. 2013b). It is thus unclear whether OSN plasticity could influence discrimination of odorants chemically different than the exposure odorant, though it is likely related to the spatial overlap between bulbar representations of unexposed odorants with an exposed odorant (Mandairon et al. 2008; Mandairon and Linster 2009). Complicating matters further, relatively few odorants have actually been employed in odorant exposure paradigms, and the limited data from genetically identified OSN populations suggests that not all such populations are equally plastic (Cavallin et al. 2010; Cadiou et al. 2014). These challenges motivated a combined study of olfactory perceptual plasticity and OSN neurophysiological plasticity to observe any changes in OSN responses to the test odors when the perceptual change is induced.

We used optical neurophysiology to observe the neurotransmitter release from populations of OSN synaptic terminals in the dorsal olfactory bulbs of adult mice during the presentation of each of 2 homologous aldehydes. These odor-evoked responses, which constitute the primary olfactory input to the brain, were assessed both before and after 7 days of exposure to a chemically different odorant (an ester), or a home-cage control period, in each mouse. To assess exposure-induced changes in odor perception, we tested whether a parallel group of mice spontaneously discriminated between these homologous aldehydes both before and after the same week-long exposure protocol that was used in the imaging experiment. We hypothesized that long-term ester odorant exposure (but not home cage control exposure) would enhance discrimination between the unexposed aldehyde pair. We also predicted that we would observe enhanced contrast between the primary sensory representations of the unexposed aldehydes after ester exposure.

Materials and methods

Subjects

Wild-type C57BL/6 mice were obtained from Charles River Laboratories (strain code #027) and were used for the habituation/dishabituation behavioral experiment. Optical imaging experiments used mice expressing the synaptopHluorin (spH) exocytosis indicator under the control of the olfactory marker protein (OMP) promoter (Bozza et al. 2004). These mice were bred on a mixed C57BL/6 × 129 background (Bozza et al. 2004) and were heterozygous for both spH and OMP. In sum, 22 adult (3–4 months), wild-type males were used in the behavioral experiment (data shown in Figure 2) and 8 adult (5–9 months) OMP-spH mice of mixed sexes were used in the optical imaging experiment (data shown in Figures 3–5).

During experimentation, subjects were singly-housed in either standard shoebox cages or custom odorant exposure chambers, as described below. Both forms of housing contained the same bedding. All animals were maintained on a 12:12-h light/dark cycle with the same food and water provided ad libitum. All experiments were performed in accordance with protocols approved by the Rutgers University Institutional Animal Care and Use Committee (Prot. #09-022).

Olfactory stimuli

An ester, *n*-butyl acetate (BA; ≥99.5% purity; Sigma–Aldrich), was selected as the exposure odorant based on previous experiments utilizing this week-long exposure paradigm (Kass et al. 2013b). Two aldehydes, heptaldehyde (HEPT; ≥95% purity; Sigma–Aldrich) and hexaldehyde (HEX; ≥98% purity; Sigma–Aldrich), were selected as discrimination stimuli for the optical imaging and behavioral experiments. These odorants were selected, in part, because they all drive input to glomeruli on the dorsal surface of the olfactory bulbs (Kass et al. 2013d), permitting in vivo visualization of odorant-evoked neural activity. Further, HEPT and HEX are aliphatic homologues (differing only in carbon chain length) that are known to be difficult

for naïve, adult mice to discriminate (Kass et al. 2013a), and thus provide an opportunity to evaluate improvement in discrimination abilities.

The relatively nonspecific perceptual effects of odorant exposure are believed to be determined by the spatial overlap between bulbar representations of unexposed odorants with an exposed odorant (Mandairon et al. 2008; Mandairon and Linster 2009), and the olfactory stimuli used here were also partly selected in accordance with this hypothesis. Qualitative comparisons between odor-evoked 2-deoxyglucose (2-DG) response maps in the Glomerular Activity Response Archive (maintained by the laboratory of M. Leon), and unpublished observations from optical neurophysiological experiments in our laboratory, indicate that the exposed and unexposed odorants do drive activity to some overlapping regions of the bulb.

For the behavioral experiment, both odorants were diluted in mineral oil in proportion to their respective vapor pressures, yielding approximately equivalent vapor concentrations (HEPT diluted to ~0.26%; HEX diluted to ~0.01%). After preparing fresh, vapor-equivalent dilutions, a photoionization detector was used to measure the concentrations of the 2 stimuli in arbitrary units (au) so that the equivalent concentrations could be calibrated on the vapor dilution olfactometer that was used during imaging. Odorant dilutions were freshly prepared each morning prior to behavioral experiments, and stimuli were calibrated from the olfactometer on the imaging rig prior to all imaging sessions via photoionization detection measurements.

Odorant exposure

As outlined in Figure 1A,B, behavioral assessments and imaging preparations were performed both before and after each mouse spent 7 days in 1 of 2 randomly assigned exposure environments. In 1 environment, mice were housed in odorant exposure chambers,

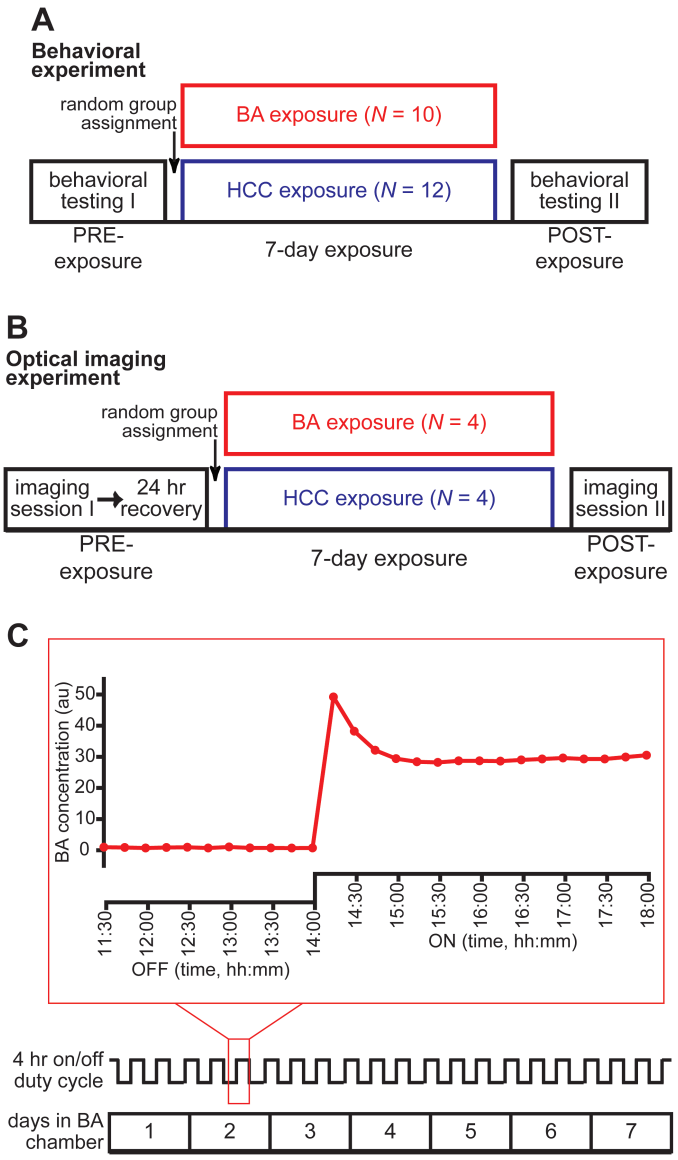

Figure 1. Summary of experimental procedures. Timeline of the behavioral (**A**) and optical imaging (**B**) experiments showing HCC and BA group assignments. (**C**) Timeline of the 7-day exposure period in a BA exposure chamber (bottom) with a trace (middle) indicating the time course of the 4-h duty cycle. The outlined portion of the duty cycle is expanded immediately above the trace (top) to show photoionization measurements that were continuously sampled once every 15 min during the last 2.5 h of an OFF cycle and then during the entire 4-h ON cycle. Animals that were assigned to the HCC group followed the same 7-day timeline, but were housed in standard cages.

and in the other, mice were housed in their (standard) home cages. Mice assigned to the latter housing environment served as the control group (home cage control, HCC).

The exposure chambers are described in (Kass et al. 2013b). Briefly, room air was pulled through the chambers by a vacuum (13 L/min), and the airflow source was shunted on a continuous 4-h duty cycle between an empty bottle (clean room air) and a bottle containing BA diluted in mineral oil. A photoionization detector was used to measure odorant concentration in the BA exposure chambers from day to day. As shown by the example measurements in Figure 1C, the sensor was also used to verify that no odor was present in the chambers during the OFF cycles, and that BA was delivered at a relatively constant concentration of ~30 au during the ON cycles.

Habituation/dishabituation behavioral assessment and analysis

To assess the perceptual similarity of HEPT and HEX both before and after the week-long exposure period (Figure 1A), we used a nonassociative, habituation/dishabituation task (Mandairon et al. 2006b, 2006c) that we have previously utilized in our laboratory (Kass et al. 2013a). In this task, after mice are behaviorally habituated to one odorant through successive presentations, they are then presented with a second odorant during a single test trial and their investigation of that second odorant is quantified and used as an index of their spontaneous discrimination between the 2 stimuli (Mandairon et al. 2006b, 2006c). If there is no perceptual difference between the 2 odorants, the mouse will continue to habituate on the test trial (as evidenced by a further reduction in investigation time). Conversely, if the odorants are perceived differently, the subject will not continue to habituate and may exhibit an increase in investigatory behavior.

Animals were housed in standard laboratory cages both before and after the exposure period, regardless of which group that they were assigned to during the week-long exposure. On testing days, the home cage was transferred from the colony room to the behavioral testing room for ~1 h prior to experimentation to allow the animals to acclimate to the transfer, and then testing was carried out in the home cage. As shown in Figure 2A, each testing session consisted of 1 trial of mineral oil (min oil) only, followed by 4 trials of HEX, and finally 1 trial of HEPT. All trials were 50 sec and presented at 5 min intertrial intervals (ITIs). During each trial a hexagonal weigh boat containing filter paper treated with 0.6 mL of solution (min oil, HEX, or HEPT, depending on the trial type) was placed on the wire cage top, and an experimenter who was blind to the experimental hypotheses used a hand-held stopwatch to score stimulus investigation time (s). Stimulus investigation was operationalized as rearing in the "odor zone," which was a clearly demarcated 15 cm × 12 cm × 10 cm, W × H × L region underlying the stimulus. Interobserver reliability of the investigation metric was confirmed in a subset of experiments where a second experimenter also scored stimulus investigation.

Baseline levels of activity were assessed by analyzing stimulus investigation during the mineral oil trial both before and after the exposure period (Figure 2C). Behavioral habituation to HEX was quantified across the 4 HEX trials in both test sessions for each subject (Figure 2B). Cross-habituation/dishabituation in each session was analyzed by comparing investigation during the last HEX trial with investigation during the HEPT (test) trial (Figure 2E,F).

All analyses shown in Figure 2B–E were performed on raw investigation time (s). The analyses shown in Figure 2F were performed on difference scores that were calculated from normalized investigation time. To evaluate relative changes in cross-habituation (or dishabituation) between the 2 odorants, we normalized investigation time for each subject within each testing session relative to the maximum time across the 4 HEX trials and the 1 HEPT (test) trial. Difference scores were then calculated for both tests from each subject by subtracting the normalized HEPT investigation from the normalized HEX4 investigation. All data (raw and normalized) were analyzed with a combination of mixed-model ANOVAs (with testing session and trial as within-subjects factors, and group as a between-subjects factor) and planned *t*-tests.

In vivo optical neurophysiology recordings

Chronic cranial windows were implanted bilaterally as previously reported (McGann et al. 2005; Czarnecki et al. 2012; Kass et al. 2013d), and can be seen in the resting light intensity (RLI) examples shown in Figure 3A,B. Briefly, mice were anesthetized with pentobarbital (100 mg/kg, ip) and dosed (s.c.) with 0.1% atropine to reduce intranasal mucous secretion. A dental acrylic head cap was fitted to the skull and permitted replicable positioning across imaging sessions. The bone overlying the dorsal surface of both olfactory bulbs was thinned, covered with a clear-drying cyanoacrylate glue to maintain transparency, and protected with a fitted metal cover in between imaging sessions. During imaging sessions, the window was topped off with Ringer's solution and a cover slip.

In vivo widefield optical imaging was performed on deeply-anesthetized OMP-spH mice, as previously described (Czarnecki et al. 2011; Moberly et al. 2012). HEPT and HEX were each delivered at their vapor-equivalent concentrations in blocks of 4–6 individual trials that were averaged together offline. Individual trials consisted of a 4-s prestimulus baseline, a 6-s stimulus presentation, and a 6-s post-stimulus recovery period, and were each separated by 60-s ITIs. HEPT- and HEX-evoked spH signals were visualized through a 4× (0.28 NA) objective on a custom-built imaging apparatus using a 470 nm LED with appropriate filters. Optical signals were recorded at 7 Hz with a 256 × 256 monochrome CCD camera (RedShirtImaging). Blank (no-odorant) trials were given throughout each preparation, and were later subtracted off-line from HEPT and HEX trials to correct for photobleaching.

Quantification and analysis of odorant-evoked optical signals

Imaging data were extracted and analyzed, as reported in (Kass et al. 2013b, 2013d). Data were processed and analyzed in Neuroplex, Matlab, and SPSS, and were subsequently graphed in SigmaPlot, Matlab, and Origin.

To generate HEPT- and HEX-evoked difference maps, the average fluorescence during 1 s immediately prior to stimulus onset was subtracted from the average fluorescence during the most typical peak odorant-evoked response. Difference maps were then spatially filtered with a low-pass median filter to correct for shot noise, and a high-pass Guassian filter to separate discrete odorant-evoked spH signals (corresponding to individual glomeruli) from broad changes in tissue reflectance (corresponding, presumably, to diffuse metabolic activity).

The raw data set for the results that are summarized by Figures 3–5 included 133 glomerular regions of interest (ROIs) from the HCC subjects and 138 glomerular ROIs from the BA-exposed subjects. Putative glomerular ROIs were first hand-selected from the spatially high-pass-filtered difference maps (examples shown in Figure 3A,B) and matched across imaging sessions for each individual subject. Then HEPT-and HEX-evoked glomerular responses

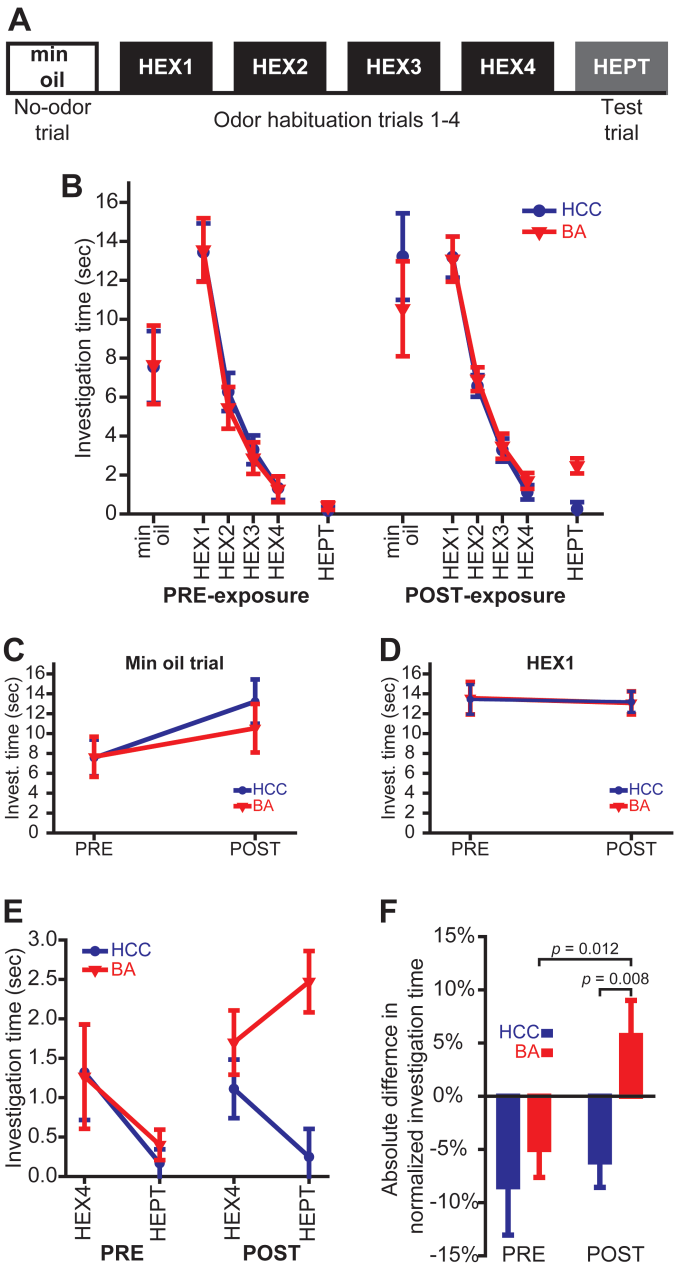

Figure 2. Chronic odorant exposure enhances olfactory discrimination abilities, but does not alter general motor activity or the propensity to investigate an odor object. (**A**) Procedure summary for the habituation/dishabituation testing protocol. (**B**) Summary of all data from PRE- and POST-exposure testing sessions. Investigation time during the mineral oil (no odor) trial (**C**) and the first habituation trial (HEX1) (**D**) before (PRE) and after (POST) the 7-day exposure period. (**E**) Investigation time during the last habituation trial (HEX4) and the test trial (HEPT) before and after HCC or BA exposure. (**F**) Difference scores (normed HEPT minus normed HEX4) for both groups during both behavioral test sessions. The data in B–F are shown as group means ± SEMs, and *P* values are by between-groups or paired *t*-tests.

were confirmed with a statistical criterion—if the mean HEPT- or HEX-evoked change in fluorescence (ΔF) across repeated trials was more than 3 standard errors greater than 0 for a glomerular ROI, then it was considered to be a response. To quantify HEPT- and HEX-evoked spH signals for traces from each pixel overlying a glomerular ROI, we subtracted the average preodorant (baseline) fluorescence from the average fluorescence during 1 s worth of frames centered on the most typical peak inflection across the traces (peak response time shown in Figure 3C,D).

To determine if there were BA-exposure-dependent changes in peak HEPT- or HEX-evoked response amplitudes, we calculated peak odorant-evoked ΔFs for all glomerular ROIs from spatially high-pass-filtered difference maps from each subject during each imaging session. To permit averaging across mice within each group, HEPT- and HEX-evoked ΔF values were then normalized within odorants across imaging sessions for each mouse, such that all evoked ΔFs per stimulus during PRE and POST were divided by the maximum evoked ΔF of PRE. The normalized ΔF values were then averaged within odorants and preps for each mouse. These data (shown in Figure 3E) were first analyzed via mixed-model ANOVA, with imaging session (pre-exposure, PRE; post-exposure; POST) and odorant (HEPT; HEX) as within-subjects factors and group (HCC;

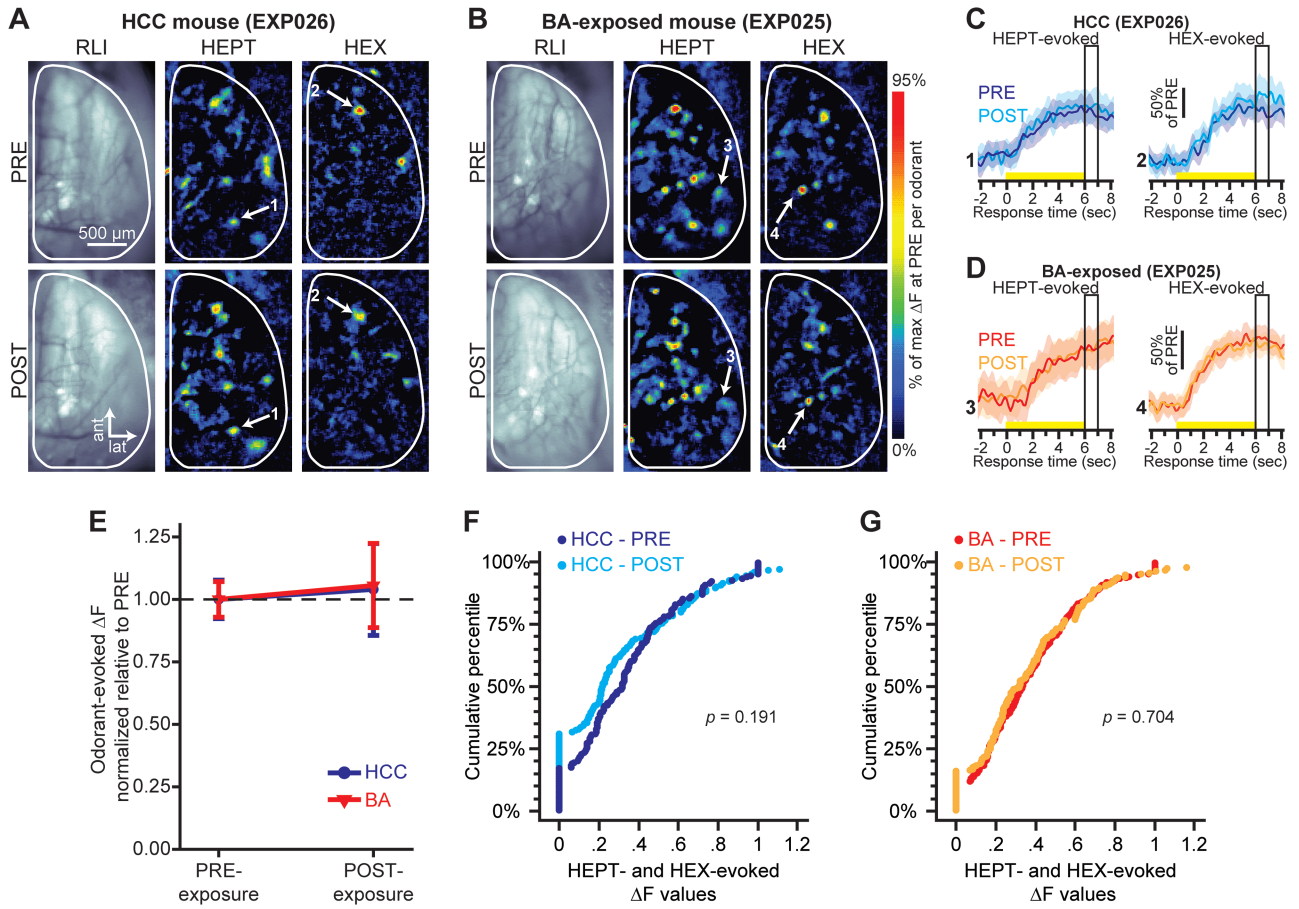

Figure 3. Peak HEPT- and HEX-evoked response amplitudes are stable over time in both HCC and BA-exposed groups. Example resting light intensity (RLI) images (left) and pseudocolored HEPT- and HEX-evoked difference maps (middle and right) from a HCC mouse (**A**) and from a BA-exposed mouse (**B**) before (top, PRE) and after (bottom, POST) the 7-day exposure period. Sets of traces from a HCC mouse (**C**) and a BA-exposed mouse (**D**) corresponding to the numbered callouts in A–B. Each set of traces was evoked by either HEPT (left) or HEX (right) both before and after the 7-day exposure period. Solid traces and surrounding shading show the mean ± SEM HEPT- or HEX-evoked spH signal across 5–6 trials. Yellow stimulus bars indicate the time of odorant presentations. Boxed regions indicate the response time corresponding to the peak odorant-evoked response maps shown in A–B and the analyses that are summarized in E–G. (**E**) Mean ± SEM normalized odorant-evoked change in fluorescence (ΔF) pooled across odorants in HCC and BA-exposed mice, and plotted as a function of the time of imaging. Cumulative probability plots showing the distributions of normalized odorant-evoked ΔF values before and after 7 days of housing in a home cage (**F**) or an exposure chamber (**G**). For each group, data are pooled across all subjects and odorants. *P* values are by Wilcoxon signed ranks test: HCC, $N_{\Delta Fs}$ = 156; BA, $N_{\Delta Fs}$ = 198.

BA) as a between-subjects factor. This analysis was then followed by planned post hoc *t*-tests. Additionally, the normalized distributions of ΔF values were pooled across glomeruli (shown in Figure 3F,G) and analyzed with Wilcoxon signed rank tests.

We next evaluated potential BA-exposure-dependent changes in the average number of glomerular responses contributing to each odor representation. As such, we quantified the number of HEPT- and HEX-evoked responses in the spatially high-pass-filtered odor maps from each subject during each imaging session. These data (shown in Figure 4A) were first tested with a mixed-model ANOVA, and then with planned post hoc *t* tests. The number of responses per odor representation does not equate to the actual frequency of odorant-responsive glomeruli because some glomeruli received OSN input that was evoked by both HEPT and HEX. To evaluate how the mouse's odor environment affected glomerular responsivity, we thus also quantified the observed frequency of glomeruli that received odorant-evoked input during PRE and POST imaging sessions. Contingency tables were generated for populations of individual glomeruli, and those contingency tables were then analyzed via χ^2 tests. Odorant selectivity (shown in Figure 4B) was also analyzed for the same populations of glomeruli by further categorizing each glomerulus as HEPT-selective, HEX-selective, or nonselective (dual, receives input evoked by both odorants), and then analyzing the resulting contingency table with log-linear regression and post hoc χ^2 tests.

Heat maps showing the patterns of spatially high-passed HEPT- and HEX-evoked activity across all glomerular ROIs from each subject were generated for both imaging sessions (examples shown in Figure 4C,D). Heat maps from each subject were normalized relative to the maximum across both odorants within each imaging preparation to visualize spatial similarity between the 2 odorants both before and after the 7-day exposure period. For further analyses on glomerular spatial representations, Pearson's correlation coefficients were calculated between peak HEPT- and HEX-evoked ΔF values that were normalized relative to the max across odorants within imaging preps (examples shown in Figure 4E,F). Correlations were performed across all individual glomerular ROIs for each subject during each imaging session.

Odorant exposure could potentially alter the temporal dynamics of OSN output to shared spatial features of the HEPT- and HEX-evoked glomerular response maps. However, because spH provides

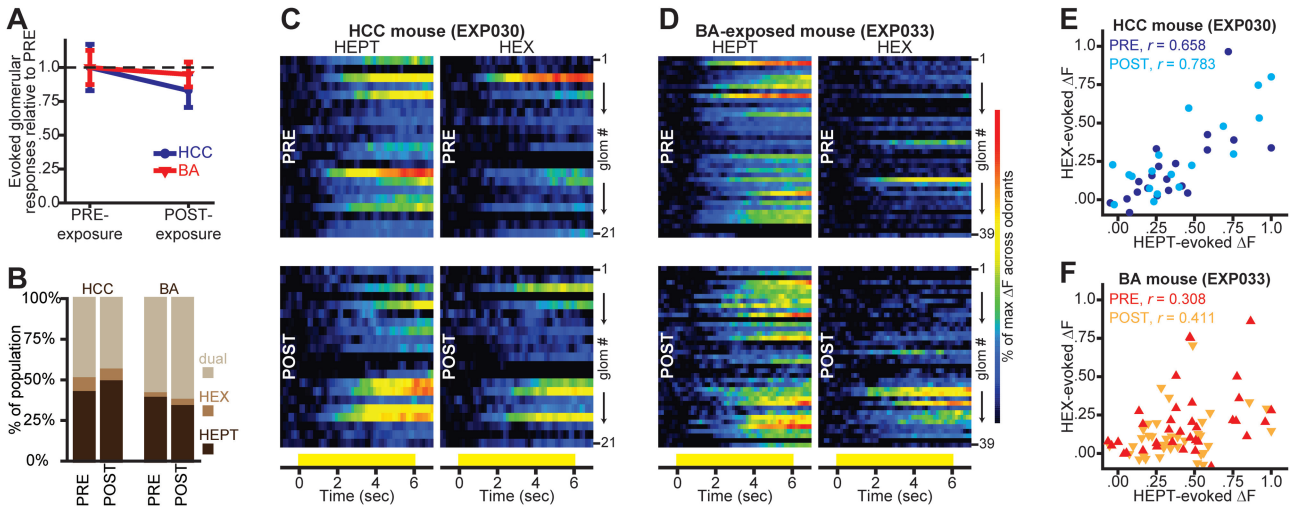

Figure 4. Aldehyde-evoked spatial maps are not altered by 1 week of HCC or ester-odorant exposure. (**A**) Mean ± SEM number of odorant-evoked glomerular responses pooled across odorants in HCC and BA-exposed mice, and plotted as a function of the time of imaging. (**B**) Percentage of HCC and BA-exposed glomerular populations that were categorized as receiving input from OSNs stimulated by HEPT-alone, HEX-alone, or by both HEPT and HEX before (PRE) and after (POST) the week-long exposure period. Pseudocolored heat maps from example HCC (**C**) and BA-exposed (**D**) mice, showing HEPT- (left) and HEX- (right) evoked activity across all glomerular ROIs PRE- (top) and POST- (bottom) exposure. Activity maps are scaled relative to the max across both odorants within each imaging session. Each row in a heat map represents the activity of a glomerular ROI (glom # 1 → *N*), and all ROIs are matched across all heat maps for each subject. Yellow bars indicate the time of odorant presentations. Scatterplots from HCC (**E**) and BA-exposed (**F**) mice showing peak HEX-evoked ΔF values plotted as a function of peak HEPT-evoked ΔF values for all glomerular ROIs shown in C–D.

an integrative signal of exocytosis over time, the peak response amplitudes (which were used in all of the analyses described previously) most frequently occur around the time of stimulus offset, and cannot inform on potential changes in temporal aspects of the nerve's output. To determine if BA exposure caused more subtle changes in the time course of HEPT- and HEX-evoked spH signals, particularly during the (relatively) early, prepeak part of the responses, all traces from glomerular ROIs were exported through custom software written in Matlab. For both PRE and POST sessions, each individual trace, which represented a single glomerulus' fluorescence throughout the length of an entire trial, was then normalized relative to the minimum and maximum across all traces within each odorant during each imaging session. To directly compare differences between the timing of HEPT- and HEX-evoked OSN responses, the normalized traces were then pooled separately for each odorant across individual glomeruli from each mouse, and were plotted relative to the individual minimum and maximum within each odorant during each preparation (examples shown in Figure 5A,B).

Results

A perceptually indiscriminable odorant pair becomes discriminable after 1 week of exposure to a single, chemically different odorant

To determine if perceptual learning occurs following our ester-odorant-exposure paradigm, we tested individual mice in the cross-habituation/dishabituation paradigm shown in Figure 2A (Mandairon et al. 2006b, 2006c) both before and after 7 days of HCC or BA exposure (Figure 1A). All data between groups and across testing sessions are summarized in Figure 2B.

There was no difference in general activity levels (as indicated by investigation during the min oil trial) between the HCC and BA groups before (Figure 2C, PRE; [independent *t* test, $t_{df = 20} = -0.041$, $P = 0.968$]) or after (Figure 2C, POST; [independent *t*-test, $t_{df = 20} = 0.812$, $P = 0.426$]) the 7-day exposure period, nor was there a change in general activity within each group between test sessions (Figure 2C; [HCC, paired *t*-test, $t_{df = 11} = -1.645$, $P = 0.128$]; [BA, paired *t*-test, $t_{df = 9} = -1.012$, $P = 0.338$]).

Overall, across both groups and testing sessions, mean ± SEM investigation time was significantly higher ($F_{1,20} = 10.894$, $P = 0.004$, $\eta_p^2 = 0.353$) during the first HEX trial (HEX1) than during the mineral oil trial (min oil, 9.741 ± 0.990; HEX1, 13.317 ± 0.765). This increase in investigation time (Figure 2B) suggests that subjects were able to detect HEX on its first presentation. Importantly, the lack of a significant testing time (PRE; POST) × trial type (min oil; HEX1) × group (HCC; BA) interaction (Figure 2B; [$F_{1,20} = 0.261$, $P = 0.615$, $\eta_p^2 = 0.013$]) and the lack of a between-groups difference during the first HEX trial alone (Figure 2D; [$F_{1,20} = 0.000$, $P = 0.995$, $\eta_p^2 = 0.000$]) confirms that the propensity to investigate an odor stimulus on its first presentation was comparable between groups and across testing sessions.

All subjects exhibited behavioral habituation across 4 presentations of HEX (Figure 2B; [main effect of trial, $F_{3,60} = 177.410$, $P \leq 0.001$, $\eta_p^2 = 0.889$]), and the rate of habituation did not differ between groups or across testing sessions (nonsignificant testing session × trial × group interaction, $F_{3,60} = 0.343$, $P = 0.794$, $\eta_p^2 = 0.017$).

During PRE-exposure testing, there was no evidence of discrimination between the 2 odorants, as all mice cross-habituated by significantly reducing their investigation time during the test trial (Figure 2E, left; [effect of trial, $F_{1,20} = 7.548$, $P = 0.012$, $\eta_p^2 = 0.274$]), regardless of group assignments (Figure 2E, left; [nonsignificant trial × group interaction, $F_{1,20} = 0.154$, $P = 0.699$, $\eta_p^2 = 0.008$]). Overall, across both groups during PRE-exposure testing, cross-habituation was thus characterized by a ~6.9 ± 2.7% decrease in odor investigation (Figure 2F, left). When subjects were tested a second time after the week-long exposure period, animals in the HCC group continued to cross-habituate, whereas the BA-exposed animals exhibited dishabituation and tended to increase their investigation times during the test (HEPT) trial (Figure 2E, right [trial × group interaction, $F_{1,20} = 8.458$, $P = 0.009$, $\eta_p^2 = 0.297$] and Figure 2F, right).

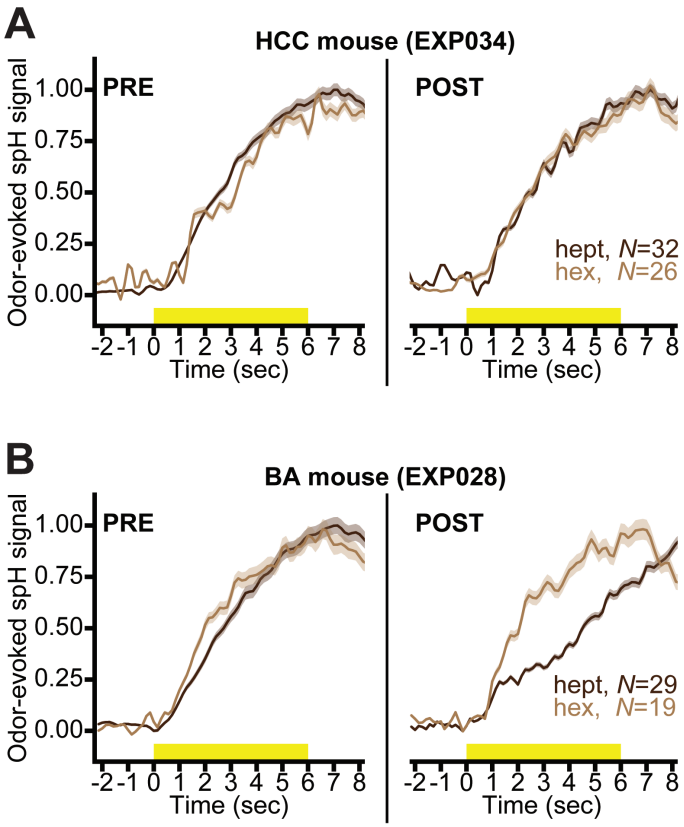

Figure 5. Ester-odorant exposure alters the temporal dynamics of activity in overlapping aldehyde-evoked glomerular response maps. Normalized HEPT- and HEX-evoked spH signals before (PRE, left) and after (POST, right) HCC (**A**) or BA (**B**) exposure. Solid lines surrounded by shading show the mean ± SEM odorant-evoked spH signals pooled across all glomerular ROIs (*N*s are indicated in each plot).

A week-long ester-odorant exposure does not alter the peak response amplitudes or overall spatial representations of 2 unexposed aldehydes

Figure 3A,B shows resting fluorescence images of the dorsal olfactory bulb through the cranial window, as well as example pseudocolored difference maps showing the pattern of HEPT- and HEX-evoked OSN synaptic input to olfactory bulb glomeruli before and after 7 days of HCC (Figure 3A) and BA (Figure 3B) exposure. As expected from the PRE-exposure (baseline) behavioral data (Figure 2E, left and Figure 2F, left), the initial neural representations of HEPT and HEX included highly-overlapping populations of OSNs—at baseline, 53% of aldehyde-responsive glomeruli (pooled across all subjects) received OSN input evoked by both HEPT and HEX. These data are consistent with the hypothesis that spatially distributed olfactory bulb representations can code for odor quality (Linster et al. 2001; Youngentob et al. 2006), and thus odorants with highly overlapping patterns of glomerular input are not spontaneously discriminated. We have observed anecdotally that spontaneously discriminated (and thus presumably perceptually dissimilar) odorants tend to have much less overlap in their glomerular representations (unpublished observations).

The effects of HCC and BA exposure on peak HEPT- and HEX-evoked response amplitudes (Figure 3C,D) were evaluated, as described previously. On average, we observed no change in the HEPT- or HEX-evoked peak ΔF for either the HCC group ($F_{1,3}$ = 0.054, P = 0.831, η^2_p = 0.018) or the BA-exposed group ($F_{1,3}$ = 0.092, P = 0.782, η^2_p = 0.030) (Figure 3C–E), nor did we observe a difference when we pooled across individual ΔF values within each imaging session for each group (Figure 3F,G).

We next found that the average number of glomeruli receiving measurable synaptic input during HEPT and HEX presentations remained unchanged after 1 week of either HCC ($F_{1,3}$ = 2.227, P = 0.232, η^2_p = 0.426) or BA ($F_{1,3}$ = 0.226, P = 0.667, η^2_p = 0.070) exposure (Figure 4A). Additionally, the observed frequency of aldehyde-responsive glomeruli (that responded to HEPT alone, HEX alone, or to both HEPT and HEX) remained stable over time in the HCC group [N_{PRE} = 99, N_{POST} = 88; χ^2 = 0.647, P = 0.421] and also in the BA-exposed group [N_{PRE} = 125, N_{POST} = 115; χ^2 = 0.417, P = 0.519]. We then assessed potential changes in the selectivity of HEPT-, HEX-, and dual-odorant-responsive glomeruli, and found that the relative frequency of glomeruli within each of the 3 selectivity categories for each group did not change across imaging sessions (Figure 4B; [nonsignificant 3-way, higher order effect, $\chi^2_{(df = 2)}$ = 1.666, P = 0.435]). Instead, aldehyde-responsive glomerular populations were best accounted for by a model with a 1-way effect ($\chi^2_{(df = 11)}$ = 232.45, $P \leq 0.001$), where the selectivity categorization itself was the strongest predictor of frequency distributions (partial, 1-way association of selectivity, $\chi^2_{(df = 2)}$ = 212.692, $P \leq 0.001$). That is, the best predictor of a glomerulus' odorant-selectivity after exposure was its selectivity before exposure.

Because BA exposure had no effect on the average number of glomeruli contributing to peak HEPT- and HEX-evoked glomerular representations (Figure 4A), or on the selectivity of individual aldehyde-responsive glomeruli (Figure 4B), the overlapping spatial features of peak HEPT- and HEX-evoked glomerular response maps probably also remained quite similar after BA (or HCC) exposure. Investigation of heat maps showing the patterns of normalized HEPT- and HEX-evoked activity across all glomerular ROIs from each subject confirm

that the spatial similarity between the 2 aldehydes was not altered by 7 days of home cage (Figure 4C) or ester-odorant (Figure 4D) exposure. Additionally, the correlation between peak HEPT- and HEX-evoked ΔFs across all glomerular ROIs for each subject was not reduced by 7 days of home cage (Figure 4E) or BA (Figure 4F) exposure, providing further evidence that the spatial similarity between the 2 aldehydes was stable over time in both groups.

Exposure to a single ester odorant can modify temporal properties of OSN responses to unexposed, aldehyde homologues and consequently enhance contrast between shared representational features

Although 7 days of ester-odorant exposure did not alter the number of glomeruli receiving aldehyde-evoked OSN input (Figure 4), or the peak response magnitude of those inputs (Figure 3), it did induce a form of perceptual learning which lead to behavioral discrimination of aldehyde homologues that were indiscriminable at baseline (Figure 2). Odor information is not solely represented by the static pattern of activity that is mapped across the glomerular layer of the olfactory bulb, but is also represented by the temporal structure of that activity (Wachowiak and Shipley 2006). Thus, although BA exposure did not change the static patterns of HEPT- and HEX-evoked activity, it could have altered the temporal dynamics of those activity patterns in a way that would enhance contrast between shared features, and that would consequently parallel the perceptual effects shown in Figure 2.

To test this, fluorescence records (traces) from all glomerular ROIs that were statistically confirmed as HEPT- or HEX-evoked responses were normalized relative to the minimum and maximum fluorescence values throughout the full trial duration and across all ROIs within each odorant-evoked activity pattern during each preparation. Because the shape of the spH waveform indicates cumulative neurotransmitter release, this analysis permitted a qualitative evaluation of the temporal structure of the HEPT- and HEX-evoked input to the brain, independent of response magnitudes and static maps. The temporal dynamics of HEPT- and HEX-evoked activity were highly similar before the week-long exposure period in HCC (Figure 5A, left) and BA-exposed (Figure 5B, left) subjects. After 1 week of HCC exposure, the time course of HEPT- and HEX-evoked activity remained relatively similar (Figure 5A, right), whereas the temporal response profiles of HEPT- and HEX-evoked activity became more distinct after BA exposure (Figure 5B, right). Although Figure 5A,B shows data from 2 representative mice, the same results were obtained when we plotted mean ± SEM traces pooled across glomerular ROIs from all subjects in the HCC (N_{HEPT} = 100; N_{HEX} = 70) and the BA-exposed (N_{HEPT} = 123; N_{HEX} = 98) groups before and after exposure. This result suggests that after BA exposure, but not HCC exposure, HEPT- and HEX-evoked neural activity become more discriminable on the basis of their temporal structures (Figure 5A,B).

Discussion

Consistent with previous reports (Mandairon et al. 2006b) we found that a perceptually indiscriminable aldehyde pair becomes discriminable to a mouse after 1 week of exposure to an ester (chemically different) odorant. Visualizing aldehyde-evoked OSN synaptic output in vivo revealed no changes in the spatial patterns of activity across olfactory bulb glomeruli after the week of odorant exposure and no change in total neurotransmitter release in each glomerulus during the 6 s odor presentation. However, we did observe that the ester exposure induced modest changes in the temporal dynamics of OSN responses to the unexposed pair of homologous aldehydes. These results are concordant with a large body of research showing that sensory enrichment can enhance neural and perceptual contrast between olfactory stimuli in a relatively nonspecific manner, and additionally show that experience-dependent modulation of olfactory temporal coding can occur in primary sensory representations.

Consistent with earlier reports (Kass et al. 2013b), we found that the number of glomeruli receiving aldehyde-evoked input from OSNs, and the peak magnitudes of those inputs, was not altered by 7 days of exposure to an ester. In the present experiments, we extended those findings to show that these odor-evoked spatial response maps remained stable, even in an exposure paradigm that successfully induced a perceptual difference between the odors. However, we did observe a modest change in the temporal dynamics of HEPT- and HEX-evoked OSN neurotransmitter release such that the timing of the odorant-evoked signal became more different between the odorants. This timing change would likely be perceptible to a mouse (Smear et al. 2013), and thus could potentially facilitate odor discrimination by downstream circuitry.

How could exposure to an ester odorant, which principally activates 1 subset of OSNs, alter the timing of the response to aldehydes in a different subset of OSNs? Odorant exposure has been reported to alter the transduction kinetics of MOR23-expressing OSNs, but not M71-expressing OSNs (Cadiou et al. 2014). It is therefore possible that ester exposure directly induced temporal changes in the odor response of some OSN populations, but not others, such that subsequent aldehyde presentation evoked more diverse timing. Alternatively, it is possible that the timing was being regulated by JG feedback at the OSN synaptic terminal, which receives strong presynaptic inhibition arising from GABAergic and dopaminergic JG circuity (McGann et al. 2005; Murphy et al. 2005; McGann 2013). The multiglomerular nature of the latter circuitry makes it an appealing vehicle for this nonodor selective effect, and this circuitry has been shown to exhibit neurochemical plasticity after odor exposure (Woo and Leon 1995; Bovetti et al. 2009; Bonzano et al. 2014).

Given the considerable evidence that static maps of peak or total glomerular activity predict the perceptual quality of an odor (Linster et al. 2001; Cleland et al. 2007), and that the difference between these maps predicts the discriminability of odors (Youngentob et al. 2006), it was perhaps unexpected that the OSN peak response maps remained unchanged while the mice began to discriminate the 2 aldehydes. In a way, the present finding that odor perception can change while the static OSN response map remains constant is the complement of a previous finding that odor perception can remain at least relatively constant whereas the OSN response map changes dramatically (Homma et al. 2009). Although the observed differences in OSN timing may certainly play a role in making the aldehyde patterns easier for the bulb to decorrelate (Linster and Cleland 2010), it is also interesting if they do not, because it suggests that later circuitry in the olfactory system can produce perceptions that at least somewhat disagree with the glomerular map. This could include lateral inhibition arising from reciprocal synaptic interactions between mitral/tufted cells and olfactory bulb interneurons (Yokoi et al. 1995; Isaacson and Strowbridge 1998). Olfactory sensory experience can refine lateral inhibition and thus sharpen odor-driven activity such that contrast is enhanced between stimulus representations, at least on some time scales (Fletcher and Wilson 2003). This contrast enhancement may be mediated, in part, through feedback circuitry between the bulb and other cortical structures. For example, the piriform cortex sends feedback to networks of

bulbar interneurons (Boyd et al. 2012), and is involved in several aspects of odor object processing that enable odor discrimination and perceptual stability (Wilson 1998, 2003; Barnes et al. 2008; Wilson and Sullivan 2011). Additionally, odor processing in piriform cortex is highly susceptible to experience-dependent modulation and correlates well with perceptual discrimination abilities (Li et al. 2008; Chen et al. 2011; Chapuis and Wilson 2012), suggesting that the exposure-induced physiological and perceptual plasticity that we observed could be mediated by cortical feedback to inhibitory bulbar networks (Boyd et al. 2012).

Activity in forebrain and brainstem transmitter systems that can modulate the inhibitory bulbar circuitry mediating lateral inhibition may also contribute to the exposure-induced perceptual and neural plasticity that we observed here. Acetylcholine, for example, has been implicated in normal odor discrimination abilities as well as in perceptual learning (Wilson et al. 2004), and pharmacologically manipulating cholinergic activity in the olfactory bulb can mimic the perceptual effects associated with odorant exposure (Mandairon et al. 2006a). Furthermore, odor-exposure-induced spontaneous discrimination between homologous esters is eliminated when a cholinergic antagonist is peripherally administered during the initial exposure period (Fletcher and Wilson 2002). An alternative mechanism for the enhanced perceptual and neural contrast that we observed between homologous aldehydes after exposure could be related to noradrenergic-mediated tuning of inhibitory circuitry in the olfactory bulb (Jiang et al. 1996; Shea et al. 2008; Linster et al. 2011; Eckmeier and Shea 2014). Similar to the exposure-induced perceptual effects reported here, noradrenergic modulation of the olfactory bulb circuitry enhances the perceptual discriminability of highly similar odorants (Escanilla et al. 2010; Linster et al. 2011), and recent work has also shown that noradrenergic input to the olfactory bulb during the time of odorant exposure is necessary for the subsequent exposure-induced perceptual learning to occur (Moreno et al. 2012; Vinera et al. 2015).

In sum, the results reported here exemplify the ability of the adult olfactory system to adapt coding strategies based on passive experience with stimuli in the surrounding environment. The underlying mechanisms for this neurophysiological plasticity may include stimulus-driven changes in the olfactory bulb circuitry mediating multiglomerular communication and lateral inhibition, as well as modulation of that circuitry by diffuse transmitter systems and top-down input from higher olfactory sensory regions.

Funding

This work was supported by The National Institute on Deafness and Other Communication Disorders [R01 DC013090 to J.P.M. and F31 DC013719 to M.D.K.]; and The National Institute of Mental Health [R01 MH101293 to J.P.M.].

Acknowledgments

We thank Michelle Rosenthal for helpful discussion on the project.

References

Altundag A, Cayonu M, Kayabasoglu G, Salihoglu M, Tekeli H, Saglam O, Hummel T. 2015. Modified olfactory training in patients with postinfectious olfactory loss. *Laryngoscope*. 125(8):1763–1766.

Barnes DC, Hofacer RD, Zaman AR, Rennaker RL, Wilson DA. 2008. Olfactory perceptual stability and discrimination. *Nat Neurosci*. 11(12):1378–1380.

Bonzano S, Bovetti S, Fasolo A, Peretto P, De Marchis S. 2014. Odour enrichment increases adult-born dopaminergic neurons in the mouse olfactory bulb. *Eur J Neurosci*. 40(10):3450–3457.

Bovetti S, Veyrac A, Peretto P, Fasolo A, De Marchis S. 2009. Olfactory enrichment influences adult neurogenesis modulating GAD67 and plasticity-related molecules expression in newborn cells of the olfactory bulb. *PLoS One*. 4(7):e6359.

Boyd AM, Sturgill JF, Poo C, Isaacson JS. 2012. Cortical feedback control of olfactory bulb circuits. *Neuron*. 76(6):1161–1174.

Bozza T, McGann JP, Mombaerts P, Wachowiak M. 2004. In vivo imaging of neuronal activity by targeted expression of a genetically encoded probe in the mouse. *Neuron*. 42(1):9–21.

Buonviso N, Chaput M. 2000. Olfactory experience decreases responsiveness of the olfactory bulb in the adult rat. *Neuroscience*. 95(2):325–332.

Buonviso N, Gervais R, Chalansonnet M, Chaput M. 1998. Short-lasting exposure to one odour decreases general reactivity in the olfactory bulb of adult rats. *Eur J Neurosci*. 10(7):2472–2475.

Cadiou H, Aoudé I, Tazir B, Molinas A, Fenech C, Meunier N, Grosmaitre X. 2014. Postnatal odorant exposure induces peripheral olfactory plasticity at the cellular level. *J Neurosci*. 34(14):4857–4870.

Cavallin MA, Powell K, Biju KC, Fadool DA. 2010. State-dependent sculpting of olfactory sensory neurons is attributed to sensory enrichment, odor deprivation, and aging. *Neurosci Lett*. 483(2):90–95.

Chapuis J, Wilson DA. 2012. Bidirectional plasticity of cortical pattern recognition and behavioral sensory acuity. *Nat Neurosci*. 15:155–194.

Chen CF, Barnes DC, Wilson DA. 2011. Generalized vs. stimulus-specific learned fear differentially modifies stimulus encoding in primary sensory cortex of awake rats. *J Neurophysiol*. 106(6):3136–3144.

Cleland TA, Johnson BA, Leon M, Linster C. 2007. Relational representation in the olfactory system. *Proc Natl Acad Sci U S A*. 104(6):1953–1958.

Czarnecki LA, Moberly AH, Rubinstein T, Turkel DJ, Pottackal J, McGann JP. 2011. In vivo visualization of olfactory pathophysiology induced by intranasal cadmium instillation in mice. *Neurotoxicology*. 32(4):441–449.

Czarnecki LA, Moberly AH, Turkel DJ, Rubinstein T, Pottackal J, Rosenthal MC, McCandlish EF, Buckley B, McGann JP. 2012. Functional rehabilitation of cadmium-induced neurotoxicity despite persistent peripheral pathophysiology in the olfactory system. *Toxicol Sci*. 126(2):534–544.

Dalton P, Wysocki CJ. 1996. The nature and duration of adaptation following long-term odor exposure. *Percept Psychophys*. 58(5):781–792.

Damm M, Pikart LK, Reimann H, Burkert S, Goktas O, Haxel B, Frey S, Charalampakis I, Beule A, Renner B, *et al*. 2014. Olfactory training is helpful in postinfectious olfactory loss: a randomized, controlled, multicenter study. *Laryngoscope*. 124:826–831.

Eckmeier D, Shea SD. 2014. Noradrenergic plasticity of olfactory sensory neuron inputs to the main olfactory bulb. *J Neurosci*. 34(46):15234–15243.

Escanilla O, Arrellanos A, Karnow A, Ennis M, Linster C. 2010. Noradrenergic modulation of behavioral odor detection and discrimination thresholds in the olfactory bulb. *Eur J Neurosci*. 32(3):458–468.

Fletcher ML, Wilson DA. 2002. Experience modifies olfactory acuity: acetylcholine-dependent learning decreases behavioral generalization between similar odorants. *J Neurosci*. 22(2):RC201.

Fletcher ML, Wilson DA. 2003. Olfactory bulb mitral-tufted cell plasticity: odorant-specific tuning reflects previous odorant exposure. *J Neurosci*. 23(17):6946–6955.

Homma R, Cohen LB, Kosmidis EK, Youngentob SL. 2009. Perceptual stability during dramatic changes in olfactory bulb activation maps and dramatic declines in activation amplitudes. *Eur J Neurosci*. 29(5):1027–1034.

Isaacson JS, Strowbridge BW. 1998. Olfactory reciprocal synapses: dendritic signaling in the CNS. *Neuron*. 20(4):749–761.

Jiang M, Griff ER, Ennis M, Zimmer LA, Shipley MT. 1996. Activation of locus coeruleus enhances the responses of olfactory bulb mitral cells to weak olfactory nerve input. *J Neurosci*. 16(19):6319–6329.

Kass MD, Moberly AH, McGann JP. 2013a. Spatiotemporal alterations in primary odorant representations in olfactory marker protein knockout mice. *PLoS One*. 8(4):e61431.

Kass MD, Moberly AH, Rosenthal MC, Guang SA, McGann JP. 2013b. Odor-specific, olfactory marker protein-mediated sparsening of primary olfactory input to the brain after odor exposure. *J Neurosci*. 33(15):6594–6602.

Kass MD, Pottackal J, Turkel DJ, McGann JP. 2013c. Changes in the neural representation of odorants after olfactory deprivation in the adult mouse olfactory bulb. *Chem Senses*. 38(1):77–89.

Kass MD, Rosenthal MC, Pottackal J, McGann JP. 2013d. Fear learning enhances neural responses to threat-predictive sensory stimuli. *Science*. 342(6164):1389–1392.

Kerr MA, Belluscio L. 2006. Olfactory experience accelerates glomerular refinement in the mammalian olfactory bulb. *Nat Neurosci*. 9(4):484–486.

Li W, Howard JD, Parrish TB, Gottfried JA. 2008. Aversive learning enhances perceptual and cortical discrimination of indiscriminable odor cues. *Science*. 319(5871):1842–1845.

Linster C, Cleland TA. 2010. Decorrelation of odor representations via spike timing-dependent plasticity. *Front Comput Neurosci*. 4:157.

Linster C, Johnson BA, Yue E, Morse A, Xu Z, Hingco EE, Choi Y, Choi M, Messiha A, Leon M. 2001. Perceptual correlates of neural representations evoked by odorant enantiomers. *J Neurosci*. 21(24):9837–9843.

Linster C, Nai Q, Ennis M. 2011. Nonlinear effects of noradrenergic modulation of olfactory bulb function in adult rodents. *J Neurophysiol*. 105(4):1432–1443.

Malnic B, Hirono J, Sato T, Buck LB. 1999. Combinatorial receptor codes for odors. *Cell*. 96(5):713–723.

Mandairon N, Didier A, Linster C. 2008. Odor enrichment increases interneurons responsiveness in spatially defined regions of the olfactory bulb correlated with perception. *Neurobiol Learn Mem*. 90(1):178–184.

Mandairon N, Ferretti CJ, Stack CM, Rubin DB, Cleland TA, Linster C. 2006a. Cholinergic modulation in the olfactory bulb influences spontaneous olfactory discrimination in adult rats. *Eur J Neurosci*. 24(11):3234–3244.

Mandairon N, Linster C. 2009. Odor perception and olfactory bulb plasticity in adult mammals. *J Neurophysiol*. 101(5):2204–2209.

Mandairon N, Stack C, Kiselycznyk C, Linster C. 2006b. Enrichment to odors improves olfactory discrimination in adult rats. *Behav Neurosci*. 120(1):173–179.

Mandairon N, Stack C, Linster C. 2006c. Olfactory enrichment improves the recognition of individual components in mixtures. *Physiol Behav*. 89(3):379–384.

McGann JP. 2013. Presynaptic inhibition of olfactory sensory neurons: new mechanisms and potential functions. *Chem Senses*. 38(6):459–474.

McGann JP, Pírez N, Gainey MA, Muratore C, Elias AS, Wachowiak M. 2005. Odorant representations are modulated by intra- but not interglomerular presynaptic inhibition of olfactory sensory neurons. *Neuron*. 48(6):1039–1053.

Moberly AH, Czarnecki LA, Pottackal J, Rubinstein T, Turkel DJ, Kass MD, McGann JP. 2012. Intranasal exposure to manganese disrupts neurotransmitter release from glutamatergic synapses in the central nervous system in vivo. *Neurotoxicology*. 33(5):996–1004.

Moreno MM, Bath K, Kuczewski N, Sacquet J, Didier A, Mandairon N. 2012. Action of the noradrenergic system on adult-born cells is required for olfactory learning in mice. *J Neurosci*. 32(11):3748–3758.

Moreno MM, Linster C, Escanilla O, Sacquet J, Didier A, Mandairon N. 2009. Olfactory perceptual learning requires adult neurogenesis. *Proc Natl Acad Sci U S A*. 106(42):17980–17985.

Murphy GJ, Darcy DP, Isaacson JS. 2005. Intraglomerular inhibition: signaling mechanisms of an olfactory microcircuit. *Nat Neurosci*. 8(3):354–364.

Shea SD, Katz LC, Mooney R. 2008. Noradrenergic induction of odor-specific neural habituation and olfactory memories. *J Neurosci*. 28(42):10711–10719.

Smear M, Resulaj A, Zhang J, Bozza T, Rinberg D. 2013. Multiple perceptible signals from a single olfactory glomerulus. *Nat Neurosci*. 16(11):1687–1691.

Valle-Leija P, Blanco-Hernández E, Drucker-Colín R, Gutiérrez-Ospina G, Vidaltamayo R. 2012. Supernumerary formation of olfactory glomeruli induced by chronic odorant exposure: a constructivist expression of neural plasticity. *PLoS One*. 7(4):e35358.

Vinera J, Kermen F, Sacquet J, Didier A, Mandairon N, Richard M. 2015. Olfactory perceptual learning requires action of noradrenaline in the olfactory bulb: comparison with olfactory associative learning. *Learn Mem*. 22(3):192–196.

Wachowiak M, Shipley MT. 2006. Coding and synaptic processing of sensory information in the glomerular layer of the olfactory bulb. *Semin Cell Dev Biol*. 17(4):411–423.

Wang HW, Wysocki CJ, Gold GH. 1993. Induction of olfactory receptor sensitivity in mice. *Science*. 260(5110):998–1000.

Watt WC, Sakano H, Lee ZY, Reusch JE, Trinh K, Storm DR. 2004. Odorant stimulation enhances survival of olfactory sensory neurons via MAPK and CREB. *Neuron*. 41(6):955–967.

Wilson DA. 1998. Habituation of odor responses in the rat anterior piriform cortex. *J Neurophysiol*. 79(3):1425–1440.

Wilson DA. 2003. Rapid, experience-induced enhancement in odorant discrimination by anterior piriform cortex neurons. *J Neurophysiol*. 90(1):65–72.

Wilson DA, Fletcher ML, Sullivan RM. 2004. Acetylcholine and olfactory perceptual learning. *Learn Mem*. 11(1):28–34.

Wilson DA, Sullivan RM. 2011. Cortical processing of odor objects. *Neuron*. 72(4):506–519.

Woo CC, Hingco EE, Johnson BA, Leon M. 2007. Broad activation of the glomerular layer enhances subsequent olfactory responses. *Chem Senses*. 32(1):51–55.

Woo CC, Hingco EE, Taylor GE, Leon M. 2006. Exposure to a broad range of odorants decreases cell mortality in the olfactory bulb. *Neuroreport*. 17(8):817–821.

Woo CC, Leon M. 1995. Early olfactory enrichment and deprivation both decrease beta-adrenergic receptor density in the main olfactory bulb of the rat. *J Comp Neurol*. 360(4):634–642.

Yokoi M, Mori K, Nakanishi S. 1995. Refinement of odor molecule tuning by dendrodendritic synaptic inhibition in the olfactory bulb. *Proc Natl Acad Sci U S A*. 92(8):3371–3375.

Youngentob SL, Johnson BA, Leon M, Sheehe PR, Kent PF. 2006. Predicting odorant quality perceptions from multidimensional scaling of olfactory bulb glomerular activity patterns. *Behav Neurosci*. 120(6):1337–1345.

Zou DJ, Feinstein P, Rivers AL, Mathews GA, Kim A, Greer CA, Mombaerts P, Firestein S. 2004. Postnatal refinement of peripheral olfactory projections. *Science*. 304(5679):1976–1979.